A finite element toolbox for the Bogoliubov-de Gennes stability analysis of Bose-Einstein condensates

Georges Sadaka[1], Ionut Danaila[1], Victor Kalt[1], Fredéric Hecht[2]

[1]Laboratoire de Mathématiques Raphaël Salem
Université de Rouen Normandie

[2]Laboratoire Jacques-Louis Lions
Sorbonne Université

09/12/2022

Introduction

Bose-Einstein Condensates (BECs)

A state of matter obtained from a dilute gas of bosons cooled to temperatures near 0 K. All particles are in the same (lowest energy) state. They are described in the Gross-Pitaevskii model by a complex wavefunction $\psi = \sqrt{\rho}e^{iS}$.

- $\rho = |\psi|^2$ corresponds to the atomic density
- $\mathbf{v} = \nabla S$ is the fluid velocity.

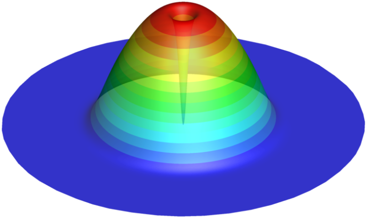

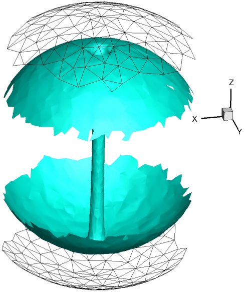

Introduction

Bogoliubov-de Gennes problem

An eigenvalue problem describing the linear stability of stationary states of Bose-Einstein condensates in the Gross-Pitaevskii framework.

Outline:

- The Gross-Pitaevskii model
- The Bogoliubov-de Gennes system
- Numerical tools
- Results

The Gross-Pitaevskii equation (GPE)

- The Gross-Pitaevskii equation (GPE), in dimensionless form:

$$i\partial_t \psi = -\frac{1}{2}\nabla^2\psi + V_{\mathrm{trap}}\psi + \beta|\psi|^2\psi \tag{1}$$

- $V_{\mathrm{trap}} = \omega_\perp(x^2 + y^2 + z^2)$: trapping potential
- β: interaction between atoms
- The GPE derives from the GP energy:

$$\mathcal{E}(\psi) = \int \left(\frac{1}{2}|\nabla\psi(\boldsymbol{x},t)|^2 + V_{\mathrm{trap}}(\boldsymbol{x})|\psi(\boldsymbol{x},t)|^2 + \frac{\beta}{2}|\psi(\boldsymbol{x},t)|^4\right) d\boldsymbol{x}. \tag{2}$$

Stationary states of the GPE

- Using the ansatz:

$$\psi(\boldsymbol{x}, t) = \phi(\boldsymbol{x})e^{-i\mu t} \tag{3}$$

- We get the stationary GPE:

$$\mu\phi = -\frac{1}{2}\nabla^2\phi + V_{\mathrm{trap}}\phi + \beta|\phi|^2\phi, \tag{4}$$

- ϕ: the stationary wavefunction
- μ: the chemical potential, related to the energy by:

$$\mu = \mathcal{E}(\psi) + \frac{\beta}{2}\int |\psi|^4 d\boldsymbol{x} \tag{5}$$

Linearization

- We linearize the GPE around the state $(\phi(\boldsymbol{x}) + \delta\phi(\boldsymbol{x}, t))e^{-i\mu t}$
- Replacing in the GPE and neglecting high order terms gives:

$$i\frac{\partial\delta\phi}{\partial t} = -\frac{1}{2}\nabla^2\delta\phi + V_{trap}\delta\phi + \beta\phi^2\overline{\delta\phi} + 2\beta|\phi|^2\delta\phi - \mu\delta\phi. \tag{6}$$

- Considering perturbations of the form $\delta\phi(\boldsymbol{x}, t) = A(\boldsymbol{x})e^{-i\omega t} + \overline{B}(\boldsymbol{x})e^{i\overline{\omega}t}$ leads yields the Bogoliubov-de Gennes eigenvalue problem:

$$\begin{pmatrix} \mathcal{H} - \mu + 2\beta|\phi|^2 & \beta\phi^2 \\ -\beta\bar{\phi}^2 & -(\mathcal{H} - \mu + 2\beta|\phi|^2) \end{pmatrix} \begin{pmatrix} A \\ B \end{pmatrix} = \omega \begin{pmatrix} A \\ B \end{pmatrix}, \tag{7}$$

where $\mathcal{H} = -\frac{1}{2}\nabla^2 + V_{trap}$

Properties of the BdG system

- If ω is an eigenvalue, then $-\overline{\omega}$ is too.
- The first eigenvalue is 0
- A non-zero imaginary part of ω indicates a dynamic instability.
- The energy difference between states ϕ and $\phi + \delta\phi$ is

$$\delta\mathcal{E} = \omega \int |A|^2 - |B|^2 d\boldsymbol{x}. \tag{8}$$

- The Krein signature $K = sign(\delta\mathcal{E})$ is linked to the energetic stability of the state

Computing the stationary state

- Use of Newton's method after separating real and imaginary parts of $\phi = \phi_r + i\phi_i$:

$$\begin{cases} \mathcal{F}_r = -\mu\phi_r - \dfrac{1}{2}\nabla^2\phi_r + V_{trap}\phi_r + \beta f(\phi_r, \phi_i)\phi_r & = 0, \\ \mathcal{F}_i = -\mu\phi_i - \dfrac{1}{2}\nabla^2\phi_i + V_{trap}\phi_i + \beta f(\phi_r, \phi_i)\phi_i & = 0, \end{cases} \tag{9}$$

  with $f(\phi_r, \phi_i) = \phi_r^2 + \phi_i^2$.
- Dirichlet boundary conditions

Computing the stationary state

- The Newton system at iteration k reads:

$$\begin{pmatrix} \left[\dfrac{\partial \mathcal{F}_r}{\partial \phi_r}\right]_{\phi_r=\phi_r^k,\phi_i=\phi_i^k} & \left[\dfrac{\partial \mathcal{F}_r}{\partial \phi_i}\right]_{\phi_r=\phi_r^k,\phi_i=\phi_i^k} \\ \left[\dfrac{\partial \mathcal{F}_i}{\partial \phi_r}\right]_{\phi_r=\phi_r^k,\phi_i=\phi_i^k} & \left[\dfrac{\partial \mathcal{F}_i}{\partial \phi_i}\right]_{\phi_r=\phi_r^k,\phi_i=\phi_i^k} \end{pmatrix} \begin{pmatrix} q \\ s \end{pmatrix} = \begin{pmatrix} \mathcal{F}_r(\phi_r^k, \phi_i^k) \\ \mathcal{F}_i(\phi_r^k, \phi_i^k) \end{pmatrix}, \tag{10}$$

where the increments are:

$$q = \phi_r^k - \phi_r^{k+1}, \quad s = \phi_i^k - \phi_i^{k+1}. \tag{11}$$

Computing the stationary state

- We solve:

$$\begin{cases} \int_{\mathcal{D}} (C_{trap} - \mu) q v_r + \int_{\mathcal{D}} \frac{1}{2} \nabla q \cdot \nabla v_r \\ \quad + \int_{\mathcal{D}} \beta \left(\frac{\partial f}{\partial \phi_r} (\phi_r^k, \phi_i^k)\, \phi_r^k q + \frac{\partial f}{\partial \phi_i} (\phi_r^k, \phi_i^k)\, \phi_r^k s + f(\phi_r^k, \phi_i^k) q \right) v_r \\ \quad = \int_{\mathcal{D}} (C_{trap} - \mu) \phi_r^k v_r + \int_{\mathcal{D}} \frac{1}{2} \nabla \phi_r^k \cdot \nabla v_r + \int_{\mathcal{D}} \beta f(\phi_r^k, \phi_i^k) \phi_r^k v_r, \\ \int_{\mathcal{D}} (C_{trap} - \mu) s v_i + \int_{\mathcal{D}} \frac{1}{2} \nabla s \cdot \nabla v_i \\ \quad + \int_{\mathcal{D}} \beta \left(\frac{\partial f}{\partial \phi_r} (\phi_r^k, \phi_i^k)\, \phi_i^k q + \frac{\partial f}{\partial \phi_i} (\phi_r^k, \phi_i^k)\, \phi_i^k s + f(\phi_r^k, \phi_i^k) s \right) v_i \\ \quad = \int_{\mathcal{D}} (C_{trap} - \mu) \phi_i^k v_i + \int_{\mathcal{D}} \frac{1}{2} \nabla \phi_i^k \cdot \nabla v_i + \int_{\mathcal{D}} \beta f(\phi_r^k, \phi_i^k) \phi_i^k v_i. \end{cases} \tag{12}$$

where v_r, v_i are the test functions.

Computing the BdG eigenvalues

- The BdG system is:

$$
\begin{cases}
\int_{\mathcal{D}} \frac{1}{2}\nabla A \cdot \nabla v_1 + \int_{\mathcal{D}} (C_{trap} - \mu) A v_1 + \int_{\mathcal{D}} 2\beta|\phi|^2 A v_1 \\
\qquad + \int_{\mathcal{D}} \beta\phi^2 B v_1 = \omega \int_{\mathcal{D}} A v_1, \\
- \int_{\mathcal{D}} \frac{1}{2}\nabla B \cdot \nabla v_2 - \int_{\mathcal{D}} (C_{trap} + \mu) B v_2 - \int_{\mathcal{D}} 2\beta|\phi|^2 B v_2 \\
\qquad - \int_{\mathcal{D}} \beta\overline{\phi}^2 A v_2 = \omega \int_{\mathcal{D}} B v_2.
\end{cases}
\tag{13}
$$

Numerical tools

- The Newton system is solved using MUMPS, GMRES and an ILU preconditioner
- Iterations are stopped by monitoring the value of the residual and the GP functional
- Mesh adaptation decreases mesh size and computation time
- ARPACK is used to compute eigenvalues and eigenvectors
- A shift $\sigma = 1e - 4$ is used when computing the eigenvalues
- The linear limit is given by:

$$\mu\phi = -\frac{1}{2}\nabla^2\phi + V_{\mathrm{trap}}\phi, \tag{14}$$

- A continuation on μ is used to follow states starting from the linear limit

Test cases

	Without adaptation			With adaptation		
	CPU time GP	CPU time BdG	mesh size	CPU time GP	CPU time BdG	mesh size
1D ground state	2	13	3602			
1D dark soliton	1	4	1356			
2D ground state	6	58	10952	12	55	10615
2D dark soliton	4801	31825	42632	2406	6014	9054
2D central vortex	838	6054	14200	596	4303	11631
3D ground state	542	4667	24576	457	3443	17831
1D dark-antidark state	1252	898	2714			
2D vortex-antidark state	1032	6498	10469	1098	5337	7874
2D ring-antidark state	2283	10353	10469	2762	10544	9533

Table: Computational time and mesh size for the different test cases. When the continuation is used, the mesh size corresponds to the last iteration.

1D ground state

- Kevrekidis and Pelinovski (2009): eigenvalues are given in the Thomas-Fermi limit by:

$$\omega_n^{\text{TF}} = \omega_z \sqrt{\frac{n(n+1)}{2}}, \quad n \in \mathbb{N}. \tag{15}$$

	$Re(\omega)$	$Im(\omega)$	K	ω_n^{TF}
ω_1	-2.89857e-15	2.16087e-07	1	$\omega_0^{\text{TF}} = 0$
ω_2	6.18933e-15	-2.16087e-07	1	
ω_3	-0.025	-8.80682e-11	1	$\omega_1^{\text{TF}} = \omega_z = 0.025$
ω_4	0.025	2.76512e-11	1	
ω_5	-0.0433018	-4.41549e-11	1	$\omega_2^{\text{TF}} \approx 0.043301270$
ω_6	0.0433018	-1.21387e-11	1	
ω_7	-0.0612394	-2.87955e-10	1	$\omega_3^{\text{TF}} \approx 0.061237243$
ω_8	0.0612394	1.64467e-10	1	
ω_9	-0.0790624	-1.09235e-10	1	$\omega_4^{\text{TF}} \approx 0.07905694$
ω_{10}	0.0790624	8.67993e-11	1	

Table: Eigenvalues and Krein signatures for the ground state in 1D

2D ground state

- Kevrekidis and Pelinovski (2009): eigenvalues are given in the Thomas-Fermi limit by:

$$\omega_{m,k}^{\mathrm{TF}} = \omega_z \sqrt{m + k^2 + 2k(1+m)}, \quad m, k \in \mathbb{N}. \tag{16}$$

	No adaptation			With adaptation			
	$Re(\omega)$	$Im(\omega)$	K	$Re(\omega)$	$Im(\omega)$	K	$\omega_{m,k}^{\mathrm{TF}}$
ω_1	-2.07687e-06	5.60174e-16	1	-6.24135e-15	1.37474e-07	1	$\omega_{0,0}^{\mathrm{TF}} = 0$
ω_2	2.07687e-06	-5.08061e-16	1	6.23144e-15	-1.37474e-07	1	
ω_3	-0.2	-4.04752e-11	1	-0.2	1.16809e-11	1	$\omega_{1,0}^{\mathrm{TF}} = 0.2$
ω_4	0.2	1.28499e-11	1	0.2	-2.51572e-11	1	
ω_5	-0.2	-9.72650e-12	1	-0.2	-5.27780e-12	1	
ω_6	0.2	-1.80613e-11	1	0.2	4.37562e-11	1	
ω_7	-0.283446	5.84768e-11	1	-0.283447	4.45534e-12	1	$\omega_{2,0}^{\mathrm{TF}} = 0.28284271$
ω_8	0.283446	6.54561e-11	1	0.283447	3.70927e-12	1	
ω_9	-0.283447	2.32827e-11	1	-0.283447	1.65992e-12	1	
ω_{10}	0.283447	2.88143e-11	1	0.283447	6.51049e-12	1	
ω_{11}	-0.348749	-3.21680e-12	1	-0.348750	1.02905e-11	1	$\omega_{3,0}^{\mathrm{TF}} = 0.34641016$
ω_{12}	0.348749	2.38853e-11	1	0.348750	1.33981e-11	1	
ω_{13}	-0.348749	-4.01642e-11	1	-0.348751	-5.37018e-12	1	
ω_{14}	0.348749	-9.62656e-12	1	0.348751	6.96459e-11	1	

Table: Eigenvalues and Krein signatures for the 2D ground state with and without mesh adaptation

2D vortex

	No adaptation			With adaptation		
	$Re(\omega)$	$Im(\omega)$	K	$Re(\omega)$	$Im(\omega)$	K
ω_1	-4.30674e-07	1.19430e-11	1	-3.57935e-07	-1.10255e-11	1
ω_2	4.30674e-07	-1.19430e-11	1	3.57935e-07	1.10255e-11	1
ω_3	-0.03276	4.34475e-11	-1	-0.03277	3.17533e-11	-1
ω_4	0.03276	-2.37988e-11	-1	0.03277	-4.42317e-12	-1
ω_5	-0.19999	3.61301e-10	1	-0.19999	-2.08322e-10	1
ω_6	0.19999	6.48508e-10	1	0.19999	-1.12710e-10	1
ω_7	-0.2	-5.65815e-11	1	-0.2	-3.17103e-10	1
ω_8	0.2	2.63500e-11	1	0.2	-2.64453e-10	1
ω_9	-0.26368	4.37599e-11	1	-0.26368	-1.31734e-10	1
ω_{10}	0.26368	-1.01262e-10	1	0.26368	-4.36461e-11	1
ω_{11}	-0.30413	7.03287e-11	1	-0.30413	-4.64402e-11	1
ω_{12}	0.30413	6.98365e-11	1	0.30413	-9.74015e-11	1
ω_{13}	-0.32627	1.20460e-10	1	-0.32628	-8.22790e-12	1
ω_{14}	0.32627	-6.03038e-11	1	0.32628	1.63267e-12	1
ω_{15}	-0.37997	-7.69693e-11	1	-0.37998	5.84810e-11	1
ω_{16}	0.37997	2.18463e-10	1	0.37998	-5.82940e-11	1

Table: Valeurs propres et signatures de Krein pour le vortex central en 2D, calculées avec le code séquentiel, avec et sans adaptation de maillage.

2D dark soliton

- State studied by Middelkamp et al. (2010)
- $|1, 0\rangle$ eigenstate in the linear limit
- Mesh adaptation every 5 iterations to limit rotation
- The anomalous mode is detected
- Dynamic instabilities correspond to collisions and bifurcations

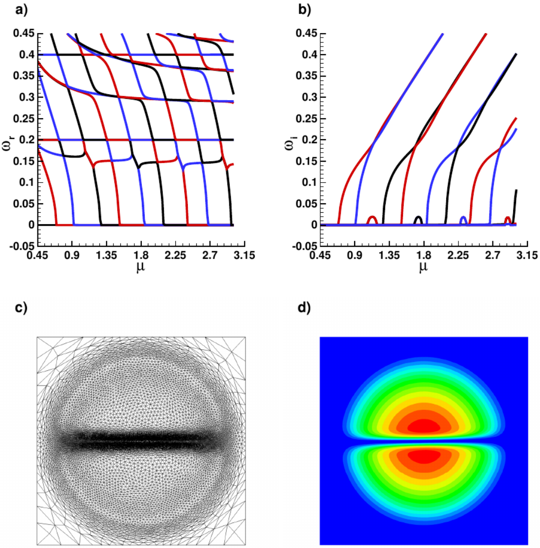

- State studied by Middelkamp et al. (2010)

$$\phi_{VS} \propto r L_0^1(\omega_\perp r^2) e^{i\theta} e^{-\frac{1}{2}\omega_\perp r^2} . e \tag{17}$$

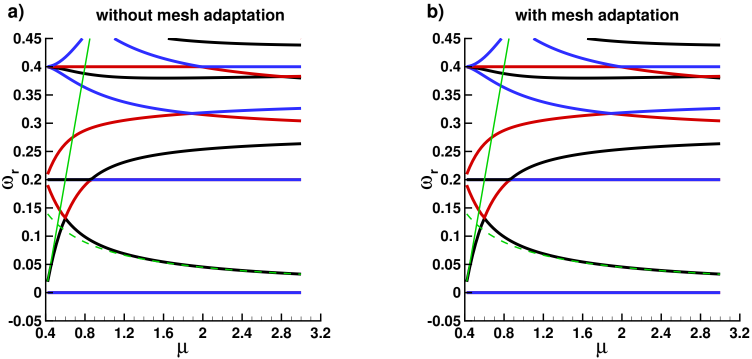

Figure: Central vortex in a 2D BEC: real part ω_r of the eigenvalues as a function of μ computed a) without and b) with mesh adaptation.

2D vortex

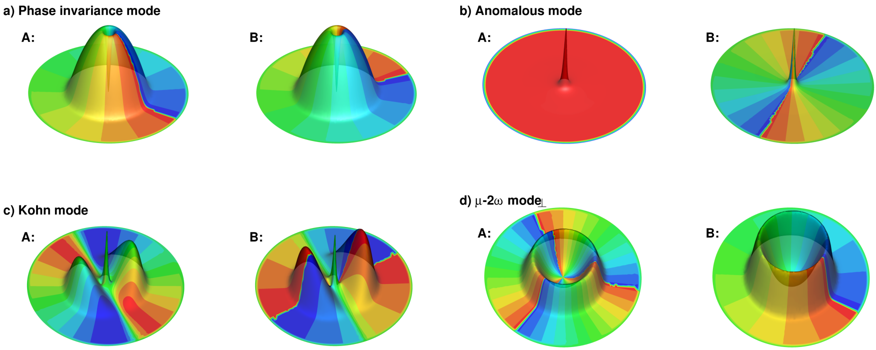

Figure: First four modes for the central vortex in a 2D BEC.

2 component BECs

- Two coupled GP equations

$$\begin{cases} \mu_1 \phi_1 = -\frac{1}{2}\nabla^2 \phi_1 + C_{\text{trap}} \phi_1 + \beta_{11} |\phi_1|^2 \phi_1 + \beta_{12} |\phi_2|^2 \phi_1, \\ \mu_2 \phi_2 = -\frac{1}{2}\nabla^2 \phi_2 + C_{\text{trap}} \phi_2 + \beta_{22} |\phi_2|^2 \phi_2 + \beta_{21} |\phi_1|^2 \phi_2. \end{cases} \tag{18}$$

- We reproduce results obtained by Danaila et al. (2016)

Dark-antidark state

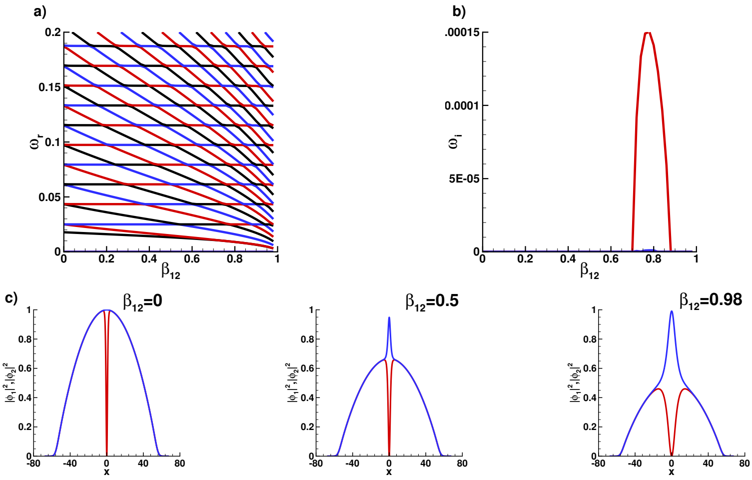

Figure: Dark-antidark state: a) real part ω_r and b) imaginary part ω_i of the eigenvalues, c) density profiles for three values of β_{12}.

Ring-antidark ring state

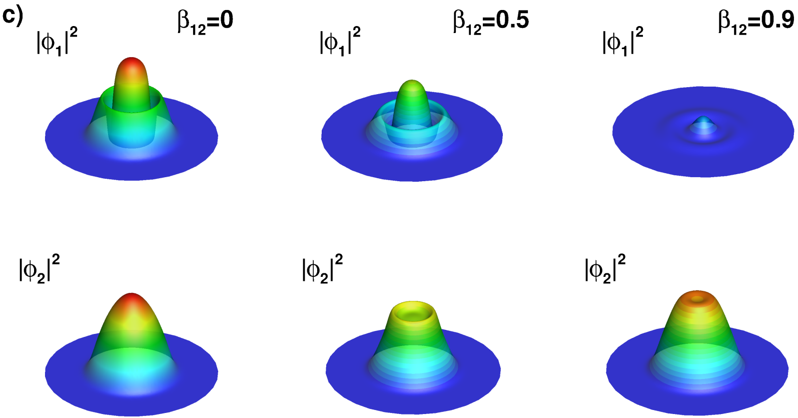

Figure: Ring-antidark ring state: density profiles for three values of β_{12}.

Ring-antidark ring state

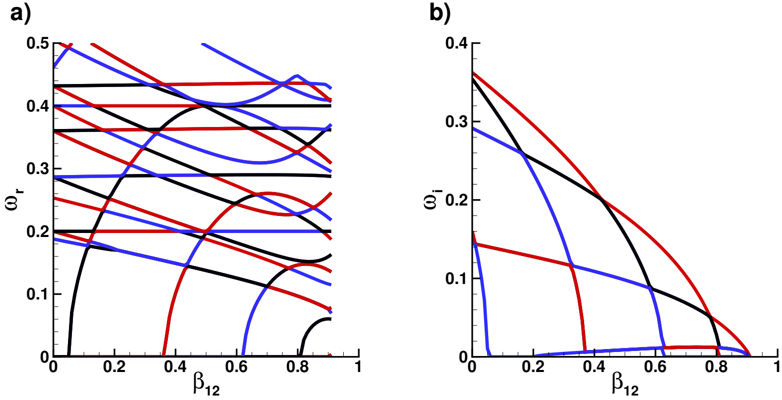

Figure: Ring-antidark ring state: a) real part ω_r and b) imaginary part of the eigenvalues.

3D states

- Only the ground state with the sequential code
- Parallel toolbox with PETSc/SLEPc (thanks to Pierre Jolivet)

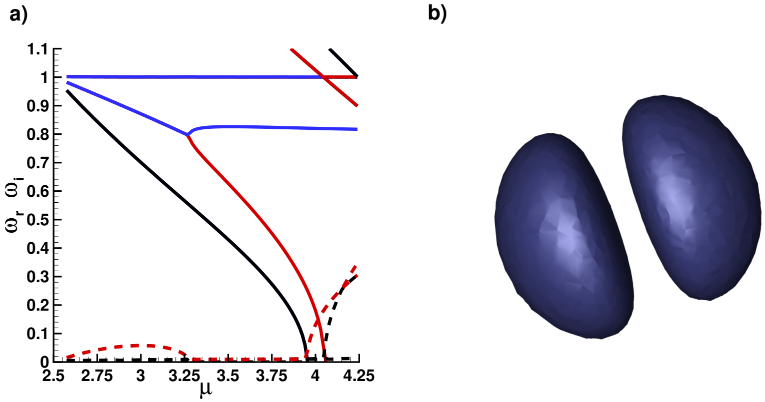

Figure: Dark soliton in 3D: a) real (full lines) and imaginary (dashed lines) parts of the eigenvalues, b) density isosurface.

Conclusion

- The code is validated against known results
- Mesh adaptation decreases the computational time

→ Study complex states in 3D with the parallel code

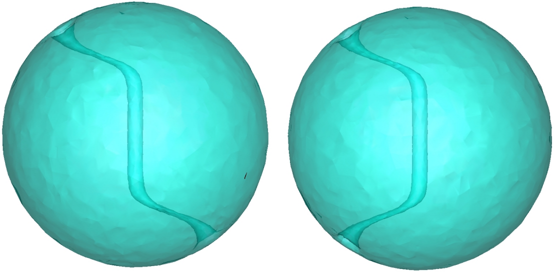

Figure: Density isosurface for S- and U-shaped vortices

Bibliography

- Kevrekidis, P.G., Pelinovsky, D.E., 2010., Distribution of eigenfrequencies for oscillations of the ground state in the Thomas-Fermi limit. Phys. Rev. A 81, 023627.
- Middelkamp, S., Kevrekidis, P.G., Frantzeskakis, D.J., Carretero-Gonzalez, R., Schmelcher, P., 2010a., Bifurcations, stability, and dynamics of multiple matter-wave vortex states. Phys. Rev. A 82, 013646.
- Danaila, I., Khamehchi, M.A., Gokhroo, V., Engels, P., Kevrekidis, P.G., 2016., Vector dark-antidark solitary waves in multicomponent Bose-Einstein condensates. Physical Review A 94, 053617.
- Bisset, R.N.,Wang, W., Ticknor, C., Carretero-Gonzalez, R., Frantzeskakis, D.J., Collins, L.A., Kevrekidis, P.G., 2015a. Bifurcation and stability of single and multiple vortex rings in three-dimensional Bose-Einstein condensates. Phys. Rev. A 92, 043601.

- **Lattice Boltzmann methods and applications**
- https://lmrs-num.math.cnrs.fr/job-postdoc-lbm-2022.html
- Contact: ionut.danaila@univ-rouen.fr